ACS APPLIED POLYMER MATERIALS

pubs.acs.org/acsapm Article

Laboratory and Field Testing Assessment of Next Generation Biocide-Free, Fouling-Resistant Slippery Coatings

Snehasish Basu, Bui My Hanh, Muhammad Hafiz Ismail, J. Q. Isaiah Chua, Srikanth Narasimalu, Manoj Sekar, Andrew Labak, Alex Vena, Philseok Kim, Teluka P. Galhenage, Scott A. Rice, and Ali Miserez*

Cite This: *ACS Appl. Polym. Mater.* 2020, 2, 5147−5162 Read Online

ACCESS | Metrics & More | Article Recommendations | Supporting Information

ABSTRACT: Recent research efforts to combat marine biofouling have focused on foul-release coatings that are not harmful for the marine environment. Inspired by nature, Slippery lubricant infused porous surfaces (SLIPS) is a surface modification technology platform with excellent antiadhesive and antifouling capacities. Precommercial coatings based on the SLIPS concept have demonstrated promising results as an environmentally friendly strategy to combat marine biofouling. Here, we investigated the resistance against marine biofouling of a range of recently developed, biocide-free SLIPS commercial coatings. The fouling resistance performance was evaluated both in the lab and in the field by conducting multimonth immersion tests in high-fouling pressure environments. In the lab, we show that the coatings are able to largely deter settlement of marine mussels—one of the most invasive marine biofouling organisms—and to weaken their interfacial adhesion strength. The key design parameter of slippery coatings to minimize fouling is the thickness of the entrapped lubricant overlayer, which can be assessed through depth-sensing nanoindentation measurements. We find that the surface energy (i.e., hydrophobic versus hydrophilic), on the other hand, does not significantly influence the antifouling performance of these coatings in lab-scale studies. After immersion in the field in stagnant waters, all coatings exhibited efficient foul-release capacity against macrofoulers, whereas under stronger hydrodynamic flow conditions, only weakly attached biofilms were detected with a bacterial community composition that is independent of the surface energy. These results suggest that these large-scale paintable coatings exhibit a strong marine biofouling resistance with low maintenance costs, which represents an important advantage from a commercial application perspective.

KEYWORDS: *foul-release coatings, marine biofouling, SLIPS, wetting properties, nanoindentation, capillary forces, field testing*

INTRODUCTION

The attachment of fouling organisms on sea-immersed structures—marine biofouling—such as shipping vessels, port and aquaculture infrastructures, or oceanographic sensors, has major economic and environmental consequences.[1,2] For example, it is estimated that the annual cost associated with biofouling on the US naval fleet alone is approximately US $180−260 million.[3] Considering that the US naval fleet represents less than 1% of vessels worldwide, the economic cost of biofouling on shipping can be extrapolated to at least US$ 30 billion per annum globally. A direct outcome of the additional fuel consumption caused by ship hull fouling is increased greenhouse emissions and their associated impact on climate change.[4] On static sea-immersed structures, hard foulers, such as barnacles and mussels, can severely damage pipelines in coastal power plants, reduce heat exchange efficiency, or even clog water distribution pipelines.[5,6] Another consequence of marine fouling is biocorrosion damage of metallic components because of metabolites produced by fouling organisms at their attachment sites,[7] which degrade submerged infrastructures.[8] Marine biofouling also has detrimental impact on coastal ecosystems as vessels are the main vectors for the translocation of invasive species out of their native environment. Prominent examples include the spread of the Asian green mussel *Perna viridis* (native to the Indo-Pacific) to the US East Coast and Australia[9] and the translocation of the fresh water zebra mussel from the Black and Caspian Seas to the North American Great Lake regions.[10,11] Both have been demonstrated to disrupt and replace native species.

Received: August 20, 2020
Accepted: September 23, 2020
Published: October 6, 2020

https://dx.doi.org/10.1021/acsapm.0c00916
ACS Appl. Polym. Mater. 2020, 2, 5147−5162

Given all of these issues, research efforts to develop coatings and paints that can prevent or at least minimize marine biofouling have been ongoing for decades, both in the lab and commercially. Fouling-resistant coatings are mostly based on two approaches:[1] (i) chemically active or antifouling (AF) coatings, which work by inhibiting or limiting the settlement of marine organisms using chemically active compounds known as biocides, and (ii) foul-release (FR) coatings, which are designed such that fouling organisms weakly attach to the surfaces, allowing their detachment through low hydrodynamic forces generated by a moving vessel.[1,6] Commercial AF paints containing the biocide tributyltin (TBT) were very successful in preventing growth of fouling organisms, but the release of TBT in marine ecosystems was later found to have severe consequences for aquatic life and human health,[12,13] eventually leading in 2003 to the ban of TBT-containing paints by the International Maritime Organization (IMO).[14] Because of this restriction, copper-containing paints have largely replaced TBT fouling-resistant coatings. However, copper (and other metal complexes) also poses problems for the environment[15] and are, thus, not a viable solution in the mid- to long-term. Additionally, a handful of biocides remain in the approved list for utilization in antifouling paint but the process of attaining regulatory approval for new biocidal compounds is lengthy and costly.

In the 2000s, enzyme-containing FR materials were also introduced but could not work effectively because of their high cost and long-term stability issues after submersion in the sea.[16] Low-cost siliconized slippery surfaces containing benzoic acid and sodium benzoate were also used for marine biofouling protection.[17] However, both were found to exhibit fast leaching from the silicone matrix.[17] TiO_2 was considered as an antifouling material, showing antibacterial activity by releasing reactive species after sunlight mediated UV exposure.[18] $CaCO_3$-containing siliconized FR materials were also developed but were shown to exhibit mass loss when immersed in water due to the dissolution of $CaCO_3$, leading to increase in roughness, which promoted macrofouling colonization.[19] Self-cleaning graphene containing silicone nanocomposite coatings have also been considered to fabricate FR materials.[20] However, graphene nanoparticles exhibit potential toxicity to marine life and decreased cell viability..[21] As a result, research efforts have heavily shifted toward biocide-free, FR coatings[1,22,23] that do not leach toxic compounds in the marine environment. Current commercial coatings are largely based on (poly)dimethylsiloxane PDMS elastomers or fluorinated polymers[23] featuring a relatively low surface energy in the range of 20−25 mN/m. The relatively weak mechanical properties and fast deterioration of these polymers have led to the development of more robust coatings, such as amphiphilic siloxane-polyurethane[24] and hybrid[25] coatings. Hydrophilic zwitterionic polymers are another class of polymers[26] that have shown some success in minimizing fouling.

A class of coatings that has recently shown encouraging success in preventing marine biofouling both in the lab and in the field are slippery liquid infused porous surfaces (SLIPS).[27,28] The design principle of these coatings is to infuse an immiscible lubricant within a porous solid surface or a three-dimensional gel network, such as PDMS.[29] Because the lubricant and the substrate have chemical affinity (either intrinsically or through chemical functionalization for porous solids) and very close surface tensions, it is thermodynamically favorable for the lubricant to remain entrapped as a thin film over the surface even after immersion in fluidic media. Additionally, for gel-based SLIPS the excess lubricant in the gel network can self-replenish the surface.[30] As a result, a thin slippery film remains on the surface, rendering it slippery and acting to mitigate biofouling through a multipronged mechanism. Indeed, slippery coatings exploit fouling-resistant strategies of both AF and FR coatings.[28] Settlement is deterred as in AF coatings—albeit through a physical phenomenon and not through the release of a biocide. In addition, the adhesion strength of foulers is minimized as in FR coatings, allowing for their easy removal at low shear stresses generated by ship movement. These mechanisms were particularly effective to avert fouling of aquatic mussels, one of the most aggressive and efficient hard macrofouling organisms.[28]

While PDMS-based lubricant-infused SLIPS are convenient for laboratory-scale and fundamental studies of the biofouling process, they are not suitable for commercial applications onto large vessels with enormous amount of surface areas. These initial prototypes were created through a postinfusion of lubricant by immersing silicone elastomer in a bath of appropriate lubricant. The lubricant then infuses into the silicone elastomer until the equilibrium is reached and maintains a slippery surface upon use. This fabrication approach is not practically feasible for large marine vessels with thousands of square meters of surface area. Indeed, marine bottom paint application has been unchanged for the last century and spray applying liquid paint is the most commonly method to apply a marine coating conformal to the bottom of the vessel. Adaptive Surface Technologies, Inc. (AST), founded to commercialize the slippery coatings technology, focuses on creating SLIPS-like surface through a curable paint formulation. As a result, the first generation of SLIPS paint was created by incorporating a chemically matched lubricant into a curable PDMS (Pt-catalyzed addition chemistry) base with a high free volume, where the lubricant is able to remain as a reservoir and migrate to the surface to create a slippery interface (SM47i-02, abbreviated SM hereafter). The lubricant was fluorinated and thus exhibited a slightly lower surface energy than PDMS, resulting in surface bloom. A second generation of coatings was optimized to (i) reduce the amount of lubricant in the coatings and (ii) minimize leaching from the coating during service by incorporating silanols and branched silane polymer that helps keeping the lubricant in the nano/micro porous surface layer of the coating. Thus, one SLIPS paint was designed with less amount of lubricant (~20% reduction compared to SM coating) using a curable PDMS based through silicone condensation chemistry (SLIPS SeaClear, abbreviated SC in the current study). Reducing the lubricant loading allows for improving the mechanical robustness and fine-tune the surface stratification of the lubricant providing slippery properties. The other coating of the second generation is a hybrid coating with amphiphilic characteristics, which was developed by incorporating a surface active polymer (SAP) within the formulation (SLIPS Foul-Protect N1, abbreviated SN in the current study). The patent pending SAP contains hydrophilic chemical moieties, which helps to broaden biofouling repellency of the coating, a drawback of low surface energy fouling release coatings given

https://dx.doi.org/10.1021/acsapm.0c00916
ACS Appl. Polym. Mater. 2020, 2, 5147−5162

the diverse adhesion preferences of 4000 plus marine organisms.[31]

In this work, all three formulations described above (SM, SC, and SN coatings) were evaluated both in the lab and in the field for long-term assessment of fouling-resistance performance. The wetting and mechanical properties of the coatings were measured by dynamic contact angle (CA) and nanomechanical methods, respectively, prior and after deployment of test panels in the field. After 6 months of immersion, we found that the surface of the coatings significantly stiffened. While depletion of the lubricant was observed, a significant amount of lubricant remained as inferred from the detection of a capillary bridge, which is the contact mechanic signature of the lubricant on the surface. As an initial evaluation of the fouling-resistance properties, we used lab-scale methods consisting of a multiple-choice coating assay allowing to evaluate whether green mussels settle on the coatings and find that all coatings can inhibit green mussels settlement, with the formulation containing the highest content of lubricant showing the best performance. The adhesion strength of mussel adhesive plaques on the coatings was on par or even below those measured for lab-scale SLIPS coatings.

For field testing, the coated panels were deployed in various locations around Singapore waters. Singapore is an ideal location to assess fouling resistance performance due to (i) the warm tropical water conditions allowing year around testing with minor variability of environmental conditions, (ii) the presence of a wide range of fouling organisms as well as their high spatial density,[32] and (iii) also it being a major shipping hub that further exacerbates fouling stresses, such as the translocation of invasive species.[33] We selected two testing sites characterized by drastically different hydrodynamic conditions. The first site was an aquaculture farm with stagnant water conditions, representative of fouling situations when a vessel is wet-docked or those occurring in static infrastructures. The second selected location featured strong tidal currents as a way to simulate hydrodynamic conditions along the hull during ship movement and, thus, better evaluate the FR performance. While settlement was observed in stagnant water conditions characterized by an aggressive fouling environment (a mussel farm), the hard foulers were readily removed from the surface, highlighting the excellent foul-release properties of the tested coatings. Under conditions of high hydrodynamic forces, low settlement biofoulers were observed after 5 months, mostly in the form of soft fouling species that could be readily removed with gentle shearing forces. The composition of biofilm communities was also obtained by metagenomic sequencing. In static water conditions, *Rhodobacteraceae* species was the most abundant, whereas under strong hydrodynamic conditions the most abundant species was *Sphingomonadaceae*, followed by *Rhodobacteraceae*. While the relative distribution of bacteria species was similar on the different types of coatings under strong hydrodynamic current conditions, we found some differences in static conditions.

MATERIALS AND METHODS

Commercial Slippery Coatings. Three commercially available coatings provided by Adaptive Surface Technologies (AST, Cambridge, USA) were tested, SM47i-02 (SM), SLIPS SeaClear (SC), and SLIPS Foul-Protect N1 (SN). The chemical formulation of SM is based on silicone binder (addition cure chemistry) and a matching partially fluorinated lubricant disclosed in Patent No. US10240067B2.[34] SC is also based on a silicone binder (condensation cure chemistry) and a matching partially fluorinated lubricant, although the amount of lubricant is reduced compared to SM since the binder system was designed to create a SLIPS with lower lubricant volume, while in principle maintaining an equivalent performance (formulation is disclosed in Patent No. US10240067B2).[34] The third coating, SN, is also a chemical formulation based on silicone binder and a matching, partially fluorinated lubricant. In contrast to SC, however, this formulation additionally contains a surface active polymer with amphiphilic characteristics as described in Patent No. US20180327684A1.[35] The additional surface-active polymer makes the surface superhydrophilic and was incorporated to further enhance the fouling release performance. For in-house (laboratory) antifouling testing, the three different coatings materials were used to coat glass slides (75 × 25 mm^2). To prepare SC and SN coated samples, base (A) and curing agent (B) were mixed in a 2:1 ratio by using a vortex (Biofrontier Technology, Singapore), whereas a 1:1 ratio was used for SM according to the manufacturer guidelines. After application of the coating on one side of glass slides, the coated samples were kept at room temperature for 24 h to obtain homogeneous SLIPS samples for further studies. PDMS and lubricant infused PDMS (PDMS) samples were prepared according to previous methodologies.[28,29]

CA Measurements. CAs were measured using a goniometer (OCA 15 Pro, DataPhysics, Germany) in ambient conditions. A 5.0 μL water droplet was pipetted onto the different coatings surfaces, and the contact angle was extracted from the software using a Young−Laplace algorithm.[36] All measurements were repeated at least five times on different areas of the substrates and averaged. CA hysteresis $\Delta\theta$ (that is, the difference between the advancing [θ_{adv}] and receding [θ_{rec}] CAs of a moving droplet) was calculated using the software SCA20. During CA hysteresis measurements, the surface was tilted with respect to the horizontal plane until the liquid droplet started to slide along the surface. The droplet profile was fitted into a spherical cap profile by the SCA20 software to determine the advancing and receding angles, as well as the sliding angle of the droplet, that is, the surface base tilt (TB) angle required to initiate the liquid droplet motion, as well as the droplet volume.

Routine Cell Culture. The RTgill-W1 (CRL-2523, ATCC) cell line, established from pieces of the rainbow trout gill filaments, was chosen as a proxy to evaluate the potential cytotoxicity of the coatings. Cells from passage numbers between 17 and 21 were used for testing. Prior to testing, cells were routinely cultured, expanded and maintained in 25 and 75 cm^2 cell culture flasks with Leibovitz's L-15 media (ATCC 30-2008) supplemented with 10% fetal bovine serum (FBS) (Gibco, USA) at 19 °C without CO_2 supplementation.

Preparation of Leachate. Prior to preparation of leachate, glass slides coated with SN was prewashed for 48 h. A total of three coated glass slides, SM, SC, and SN were soaked in 45 mL of ultrapure water (PURELAB flex 3, Veolia, UK) for 1 week at room temperature, allowing any leachate to dissolve into the water. After soaking, the water containing leachate was freeze-dried, resuspended in complete L-15 medium, and put into a 37 °C incubator for 1 h to allow the leachate to dissolve into the medium. The assay media were prepared for test surfaces (SM, SC, and SN), cell death negative control (media only) and cell death positive control (1% Triton-X). The assay medium was passed through a 0.2 μm syringe filter before use in the toxicity assay.

Cell Culture Preparation for Toxicity Assay. For exposure to the assay media, confluent RTgill-W1 cells were washed twice with PBS (Gibco, USA), detached with 0.25% trypsin (Gibco, USA) by incubating for 5 min at 37 °C, pelleted at 200 × *g* for 5 min, and resuspended in 1 mL complete L-15 medium. The cell density was determined using the Countess II Automated Cell Counter (Invitrogen, USA) and diluted to 300 000 cells/mL before being seeded into 48-well multidishes (Nunclon, USA). The cells were allowed to attach for 24 h before the L-15 medium was replaced by the assay medium.

https://dx.doi.org/10.1021/acsapm.0c00916
ACS Appl. Polym. Mater. 2020, 2, 5147−5162

Cytotoxicity Test. To determine toxicity of the surfaces, a combination of 2 methods was used. The alamarBlue cell viability reagent (Invitrogen, USA) utilizes the reducing power of living cells as an indicator of cell health, and the LDH Cytotoxicity Detection Kit (Takara Bio, USA) detects for lactate dehydrogenase that is released into cell culture supernatant during cytoplasmic membrane damage. Briefly, after 24, 48, and 72 h, the assay medium was transferred to a clean 48 well multidish for use with the LDH detection kit while the cells were washed gently with 1 × PBS before testing with alamarBlue. For the alamarBlue test, 526 μL of alamarBlue was added to 10 mL of complete L-15 medium before 300 μL of the solution was added to the assay wells. The cells were incubated for 1 h, protected from light, before the fluorescence was measured from each well at excitation/emission wavelengths of 530/590 nm, respectively, in a microplate reader (Infinite 200 PRO, Tecan, Switzerland). For LDH detection, the transferred cell culture supernatant was centrifuged at 250 × *g* for 10 min. From each well, 100 μL of supernatant was transferred each to 3 wells of a 96-well multidish (Nunclon, USA) before the test was performed as per the manufacturer's instructions. The absorbance at 490 nm was measured in a microplate reader (Infinite 200 PRO, Tecan, Switzerland).

Surface Energy. Deionized water, ethylene glycol (Sigma-Aldrich, USA) and diiodomethane (Sigma-Aldrich, USA) have well-known surface tension values.[37] These standard liquids were used to determine the surface energy (SE) of all samples using the Owens, Wendt, Rabel, and Kaelble (OWRK) method,[38] which is based on the geometric mean approach to combine dispersion and polar components for the calculation of SE using eq 1:

$$\gamma = \gamma^d + \gamma^p \quad (1)$$

where γ is the total surface free energy, and γ^d and γ^p are the dispersion and polar components of the surface energy, respectively.

Mussel Collection and Preparation. Green mussels (*Perna viridis*) were obtained from an aquaculture farm located off Lorong Halus Industrial Park, Singapore (same location as for the field testing described below). Adult mussels of 4−5 cm in length were selected and thoroughly cleaned using seawater. The mussels were immediately placed in shallow tanks of an artificial seawater aquarium system and equilibrated for 3 days at constant running seawater prior to the experiments. For the entirety of the test, the water was kept at an optimum temperature of 27−29 °C, pH 7.9−8.1, and a specific gravity between 1.022 and 1.023. In our checkerboard assays and adhesive strength testing described below, live mussels were regularly scattered on the test surfaces at the beginning of the assay.

Checkerboard Mussel-Choice Assays. To assess the mussel's preference for substrates, a checkerboard assay with randomly positioned substrates was conducted according to our previous design.[28,39] One checkerboard (5 × 6) contained all three coatings (SM, SC, and SN) plus PDMS and silicon oil infused PDMS (iPDMS) as control substrates. The two additional checkerboards (10 × 3) were prepared with only the commercial coatings to directly compare their performance without introducing additional bias. The checkerboards were mounted on solid supports to prevent the mussels from exploring other surfaces from the seawater tanks. A total of 20 mussels was placed on each of the checkerboards, which were immersed in continuous running artificial seawater (27 °C, pH 8.0, and specific gravity ∼ 1.023). The behavior of mussels was observed for one month and the total number of adhesives plaques planted on each coated surface was counted at the end of the assay.

Adhesive Strength Measurements. A customized microtensile machine was used to measure the pull-off force (plaque/substrate separation−force) of individual mussel plaques as described in our previous studies.[28,39] The tensile tester was equipped with a 100 g load cell (Futek, USA). Mussel byssal threads were cut with a clean sterile razor from the mussel proximal end and were kept hydrated in seawater prior to the measurements. All threads attached on the SLIPS surfaces (SM, SC, and SN) were pulled at an angle of 90° ± 5° relative to the surface, and the plaque orientation relative to the thread remained the same for all threads. The pulled-off plaque traces were subsequently marked, and their areas were measured using an optical microscope (Axio Scope.A1, Zeiss) equipped with an imaging software (AxioVision version 4.8.2, Zeiss). The adhesion strength on each test surface was measured by using the maximum applied load at failure divided by the plaques' areas. For all surfaces, the adhesion strength tests were conducted on threads deposited on samples from at least five mussels and the mean value of all data was reported.

Nanoscale Contact Mechanics Experiments. Two types of experiments were conducted using a Triboindenter TI-950 nanomechanical tester (Hysitron, USA) to assess the contact mechanic characteristics of the SM, SC, and SN surfaces. For the infused surfaces, cono-spherical tips with nominal radii of 10 (elastic modulus measurements) and 50 μm (capillary adhesion force measurements) were employed, together with an extended displacement stage allowing to impose maximum displacements of up to 500 μm. A transducer with maximum force of 12 mN was used for the force measurements. To detect the "jump-in/jump-off" effect and capillary bridging, "air-indent" experiments in the imaging mode were conducted as described before.[28,39] In these experiments, the imaging mode of the equipment is used to record any force jump associated with the contact event, which produces a "jump-in" effect[28] as the capillary bridge pulls on the tip. The extracted unloading curve was used to obtain the capillary adhesion force (maximum negative force measured during the unloading segment of a loading/unloading cycle), whereas the elastic modulus of the infused samples was obtained by fitting of the loading portion of loading/unloading curves using the Hertzian equation.[40]

Preparation of Coated Surfaces for Field Testing. To investigate the fouling resistance performance of the coatings in immersed sea environments (field studies), seven types of samples were prepared on aluminum plates measuring 10 × 15 mm^2: 3 commercial coatings (SM, SC, SN), PDMS and iPDMS, as well as primer (Intershield Primer 300, AkzoNobel, Singapore) and tie-coat (Tie-coat Intersleek 731 AkzoNobel, Singapore) paints as additional controls. SM was prepared separately on aluminum plates precoated with Intershield Primer 300. SC and SN were prepared on aluminum plates precoated with Intershield Primer 300 followed by Tie-coat 731, respectively. PDMS was cured on the aluminum plate at 70 °C for 4 h and infused by using 10 μL/cm^2 silicon oil (10 cSt Trimethylsiloxy terminated, Gelest) to make iPDMS samples.

The field studies were conducted in two sites exhibiting very different hydrodynamic flow conditions. For testing in static water conditions, the coated plates were fixed to a plastic frame (Figure S1a) and submerged (Figure S1b) for 6 months in an aquaculture farm near Lorong Halus off the North-East coast of Singapore (1.2244° N; 103.5539° E). The plastic frame was immersed at a depth of approximately 1.5 m during low tide, in an open-water pool used for green mussel farming. Subsequently, the exposed surfaces were inspected for settlement and growth of fouling organisms after 9, 20, 32, 46, 74, 100, and 190 days, respectively. Testing under stronger hydrodynamic conditions was carried out at the Sentosa boardwalk, Singapore (1.2601° N; 103.8232° E), which is subjected to strong tidal currents ranging from 0.7 to 1.3 m/s as the tidal flow changes every 6 h. All seven coatings were prepared as mentioned above and fixed to a custom-based aluminum frame (Figure S2a) designed to resist the large hydrodynamic stresses generated by tidal currents. The frame was submerged (Figure S2b) at a depth of approximately 1.5 m during low tide for 5 months (which was the period during which the testing site was allowed to be accessed). Inspection of the exposed coated surfaces was carried out after 20, 70, and 150 days, respectively.

Ribotyping. Samples were obtained from the Lorong Halus and Sentosa sites at the sixth and fifth month respectively using sterile cotton swabs. Total genomic DNA was extracted from the swabs using the DNeasy Power Biofilm Kit (Qiagen, Germany) as per manufacturer's instruction. The V4 region of the 16S small subunit

https://dx.doi.org/10.1021/acsapm.0c00916
ACS Appl. Polym. Mater. 2020, 2, 5147−5162

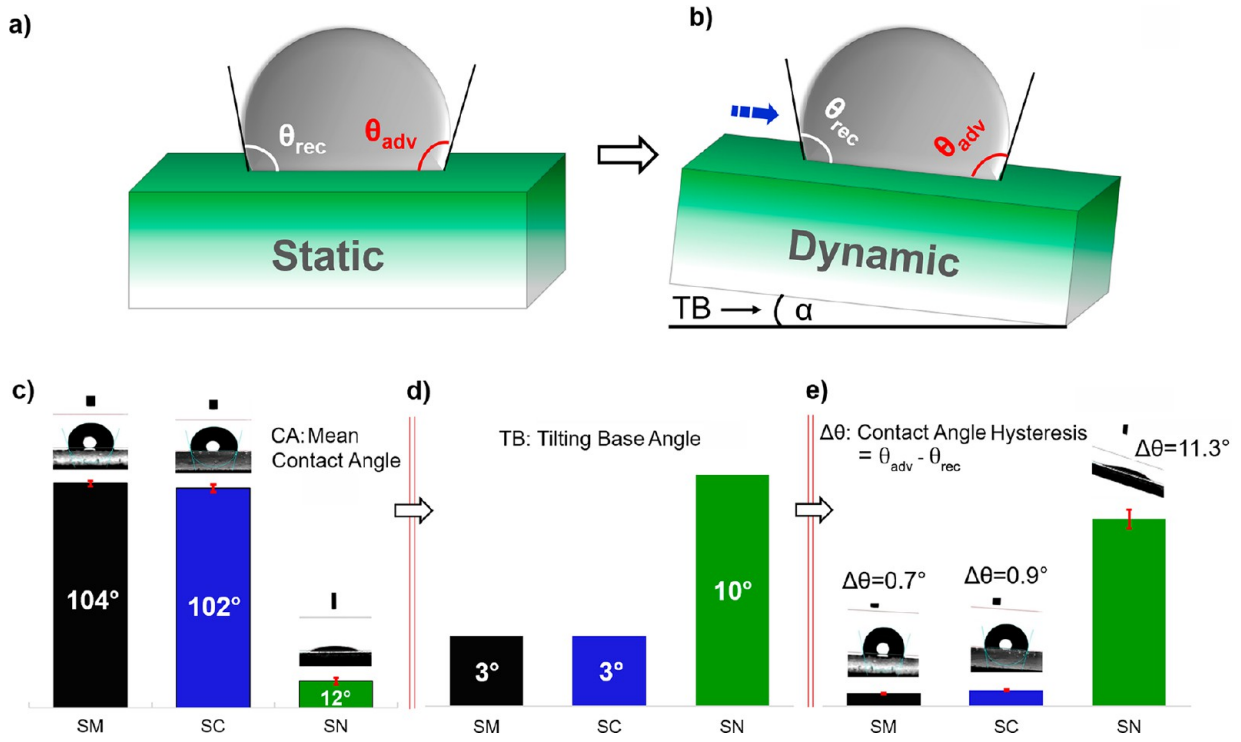

Figure 1. Static and dynamic water contact angle (CA) measurements of SM, SC, and SN SLIPS coatings. (a, b) Schematic representation of static (a) and dynamic (b) water droplet measurements. (c) Mean CA of static water droplets. (d) Tilting base (TB) angle of mobile water droplets, corresponding to the tilting angle at which droplets start to slide along the surface. Droplets were allowed to slide for 25 s at the specific TB angle of each coating. (e) Contact angle hysteresis ($\Delta\theta = \theta_{adv} - \theta_{rec}$) of mobile water droplets, where θ_{adv} is the advancing contact angle and θ_{rec} is the receding contact angle.

was amplified using primer sequences containing Illumina-specific overhangs, F:5′GTGCCAGCMGCCGCGGTAA and R:3′GGACTACHVGGGTWTCTAAT,[41] and Q5 polymerase with the following cycling conditions: (i) initial denaturation at 98 °C for 30 s; (ii) 35 cycles of 98 °C for 10 s, annealing at 50 °C for 30 s, extension at 72 °C for 30 s; and (iii) final extension at 72 °C for 2 min. The amplicons were purified using the AMPure XP PCR purification magnetic beads (Beckman Coulter, USA) as per manufacturer's instruction and then sequenced on an Illumina MiSeq as 300 bp paired end reads with a 20% PhiX spike-in.

The sequences were primer and adapter removed using cutadapt v 2.4 before being used for processing using DADA2 v 1.14.1.[42] Briefly, the sequences were filtered to remove PhiX and truncated to remove low quality bases, the sequence variants were inferred, merged, chimeras removed, and had taxonomy assigned, followed by analysis using phyloseq v 1.30.0.[43] Statistical analysis was done using the vegan v 2.5−6 package.[44]

RESULTS

Surface Characterization. Static and dynamic CA measurements of SC, SM, and SN coated surfaces were carried out to analyze their wetting and slippery properties (Figure 1). Under static conditions (TB angle = 0°, Figure 1a), SC and SM surfaces exhibited hydrophobic properties with a mean CA larger than 100° (Figure 1c, Table 1) and similar surface energies of 23.4 mN/m (SC) and 23.7 mN/m (SM) (Table 1). The uniformity of the infused slippery coatings was evaluated by measuring $\Delta\theta$ using dynamic water CA measurements (Figure 1b) at a specific TB angle (Figure 1d), which provides the resistance to droplet mobility. $\Delta\theta$ values below 2.5° are considered ideal to restore liquid repellency after physical damage (within 0.1−1 s), resulting in a nonsticking surface with a lack of pinning because the surface can be considered as essentially defect-free.[45,46] On both SM and SC surfaces, water droplets rolled at a low TB angle (3°), suggesting that these surfaces were extremely slippery and hydrophobic. Their slippery nature was confirmed by a very low $\Delta\theta$ value of 0.8 ± 0.1° (Figure 1e). In contrast, the SN was much more hydrophilic as expected with a mean CA of 12° (Figure 1c, Table 1) and a high surface energy of 58.3 mN/m (Table 1), about 2.5-fold larger than SM and SC coatings. This resulted in water droplets rolling at a higher TB angle of 10° (Figure 1d), with a contact angle hysteresis $\Delta\theta \approx 11.3°$ (Figure 1e).

Table 1. Wetting Properties of the Coatings[a]

sample	CA (deg)	$\Delta\theta = \theta_{adv} - \theta_{rec}$ (deg)	TB angle (deg)	surface energy (mN/m)
SN	12.0	11.3	10	58.3
SC	102	0.9	3.0	23.7
SM	104	0.7	3.0	23.4

[a]CA: Contact angle, $\Delta\theta$: Contact Angle hysteresis, TB: Tilting Base angle.

Long-Term Stability of the Coatings in Air and Water. CA measurements were also conducted on coated SLIPS samples (SM, SC, and SN) kept in ambient conditions for 1 year as well as immersed in seawater for 5 months followed by 1 month in air. There were no significant in water CAs differences for the hydrophobic (101−104°) SM and SC coatings (Figure S3) for all conditions. While the CA (12°) of the hydrophilic SN coating did not vary over time when kept in air, it increased to 79° after being immersed in seawater for 5 months (Figure S3). This observed change in CA of SN is attributed to the rearrangement of hydrophilic

https://dx.doi.org/10.1021/acsapm.0c00916
ACS Appl. Polym. Mater. 2020, 2, 5147−5162

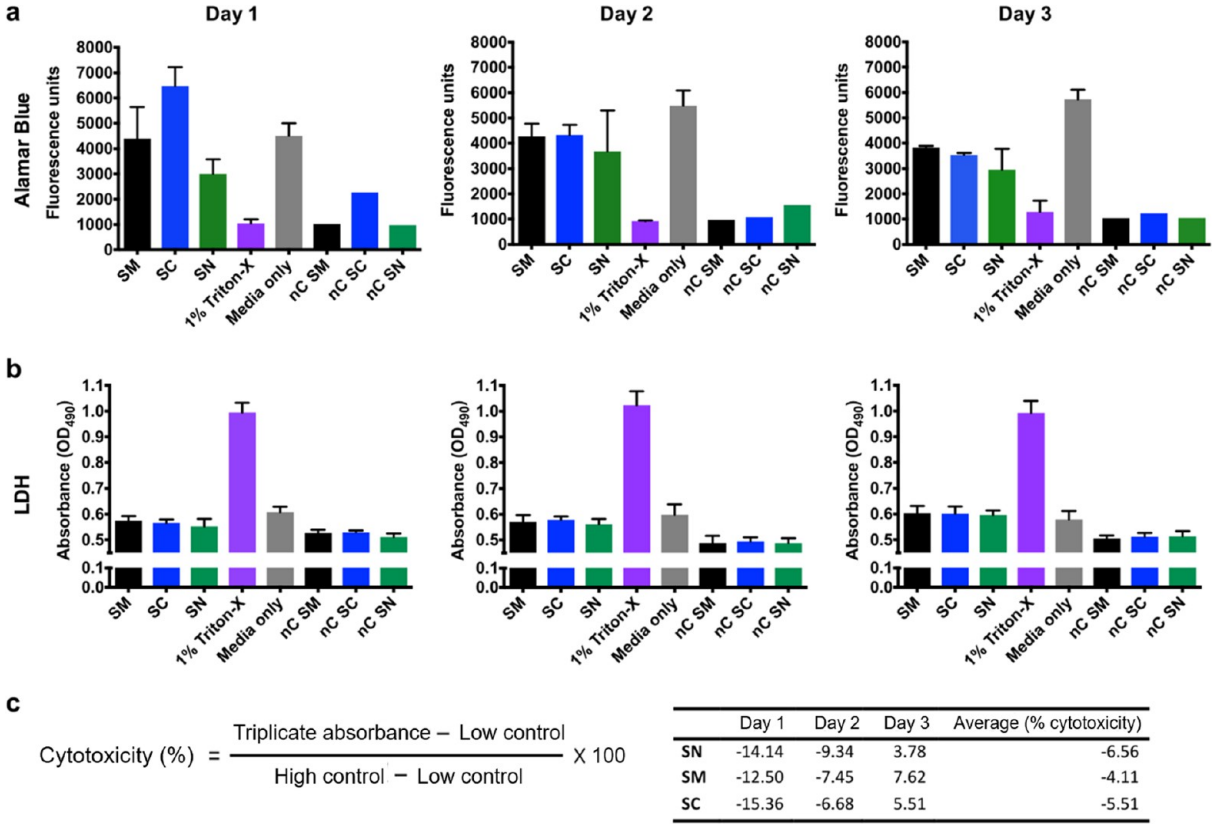

	Day 1	Day 2	Day 3	Average (% cytotoxicity)
SN	-14.14	-9.34	3.78	-6.56
SM	-12.50	-7.45	7.62	-4.11
SC	-15.36	-6.68	5.51	-5.51

Figure 2. Assessment of cytotoxicity of the leachate from the surfaces. Rainbow trout gill cells RTgill-W1 were exposed to assay media containing leachate prepared from SM (black), SC (blue), and SN (green), for up to 3 d (72 h). The controls were complete L-15 medium supplemented with 1% Triton-X (violet) as a positive control (+) for cell death, and complete media only (gray) as a no killing control (−). There were also no cell controls representing background signals from the test solutions. Cell viability measured cellular metabolic activity using the alamarBlue assay (a) and plasma membrane damage using the LDH assay (b). The cytotoxicity of the leachate (c) was calculated from the LDH assay values. All values obtained were a mean of 3 technical replicates except for the no cell control of the alamarBlue assay, and the error bars are the standard deviation of the values obtained.

and hydrophobic domains of the coating with exposure to seawater as amphiphilic coatings are known to show such rearrangement behavior.

Cytotoxicity of Commercial SLIPS. The coated surfaces were tested for toxicity against rainbow trout gill cells as a relevant proxy for organisms present in marine waters[47] and done similarly in a recent study.[39] The assays suggested that all the surface types were not toxic to the fish gill cells, with the cells showing higher metabolic activity than the cell death positive control and comparable LDH levels to the media-only cell death negative control (Figure 2). This includes the SN coating that was soaked in water for 48 h to leach out unreacted amphiphilic chemicals used in the coating formulation, indicating that this preconditioning treatment was sufficient to remove potentially cytotoxic residual chemicals from the coatings.

Nanoscale Contact Forces. Beyond surface energy considerations, biofouling is also linked to the mechanical and physicochemical properties of the coating, namely the elastic modulus and, in the case of slippery coatings, capillary forces arisen at the coating/fouler interface due to the lubricant layer. To measure the elastic modulus on the surface of the coatings, we carried out depth-sensing nanoindentation measurements using a spherical indenter geometry with a 10 μm nominal radius, and the modulus was obtained by fitting the load−displacement curves with the Hertzian equation[40] up to ∼3 μm contact depth. Characteristic load−displacement curves on fresh samples (before immersion in the field) are shown in Figure 3a and b. SC contains the lower lubricant loading during preparation and it was the stiffest among all coatings, with an elastic modulus of 0.62 ± 0.04 MPa, compared to 0.29 ± 0.02 for the SN coating and 0.16 ± 0.03 MPa for the SM coating, respectively (Figure 3a, Table 2). For swollen networks, such as lubricant-infused elastomers in this study, the elastic modulus is inversely proportional to the swelling ratio,[48] which should increase with the volume of lubricant. These results are, thus, consistent with the higher relative volume of lubricant used in the SM coating formulation.

The second critical property measured by depth-sensing nanoindentation is the capillary force occurring at the solid/lubricant interface. Indeed, it was previously suggested that a central design criterion of slippery coatings to inhibit mussel fouling is the presence of a capillary bridge at the interface that can mask the surface from the mussel foot (the organ used to sense the surface and subsequently secrete threads), in turn disrupting the byssal thread secretion process.[28] In a depth-sensing nanoindentation experiment, a capillary bridge is inferred when an adhesive force is measured during the retraction step from the surface, as shown in Figure 3c−f (schematic illustrated in the inset of Figure 3c). Whereas the capillary adhesive forces between SC, SM, and SN surfaces were nearly equivalent ($F^{\#} \sim 13-16$ μN), we measured much longer capillary bridges for fresh SM ($H^{\#}_{SM}$ = 32.5 μm; Figure

https://dx.doi.org/10.1021/acsapm.0c00916
ACS Appl. Polym. Mater. 2020, 2, 5147−5162

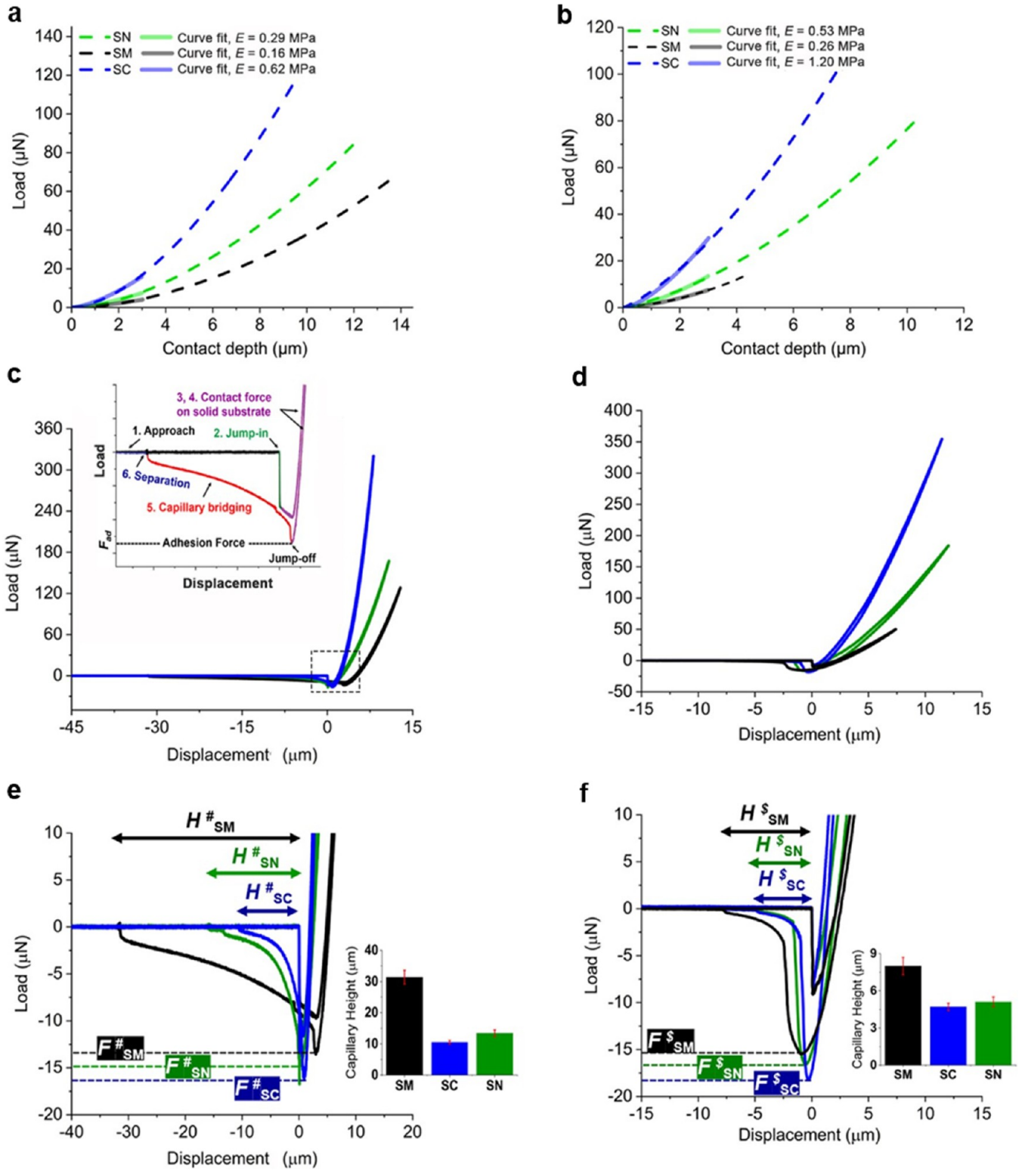

Figure 3. Nanoindentation measurements of SC, SM, and SN coatings. (a, b) Load−displacement curves obtained with a conospherical tip (10 μm radius). The elastic modulus was inferred from the loading portion of a loading/unloading cycle using the Hertzian solution on fresh samples (a) and after 5 months of immersion in the field (high hydrodynamic current conditions) (b). (c, d) Characteristic load−displacement curves obtained with a conospherical tip (50 μm nominal radius) used to detect capillary forces on fresh samples (c) and after 5 months of immersion in the field (d). Inset in panel c is a zoom-in view of a representative curve showing the different steps when a capillary force is detected. (e, f) Enlargement of the capillary adhesive force ($F^{\#}$ and $F^{\$}$) regimes of fresh samples (e) and after 5 months of immersion in the field (f). #: Fresh samples. $: After 5 months of immersion in the field.

3e, Table 2) compared to SC and SN surfaces (10−13 μm; Figure 3e, Table 2), suggesting that SM has a thicker lubricant overlayer among all slippery coatings, which initially provides better shielding against detection of the surface by

https://dx.doi.org/10.1021/acsapm.0c00916
ACS Appl. Polym. Mater. 2020, 2, 5147−5162

Table 2. Nanoscale Characterization of the Coating

sample	modulus[#] (MPa)	modulus[$] (MPa)	capillary height ($H^{\#}$) (μm)	capillary height ($H^{\$}$) ($\mu$m)	adhesion force ($F^{\#}$) (μN)	adhesion force ($F^{\$}$) ($\mu$N)
SN	0.29	0.53	13.4	5.1	14.7	16.6
SC	0.62	1.20	10.5	4.7	16.2	17.5
SM	0.16	0.26	31.4	8.0	13.0	15.4

[#]Fresh samples. [$]Sea immersed samples.

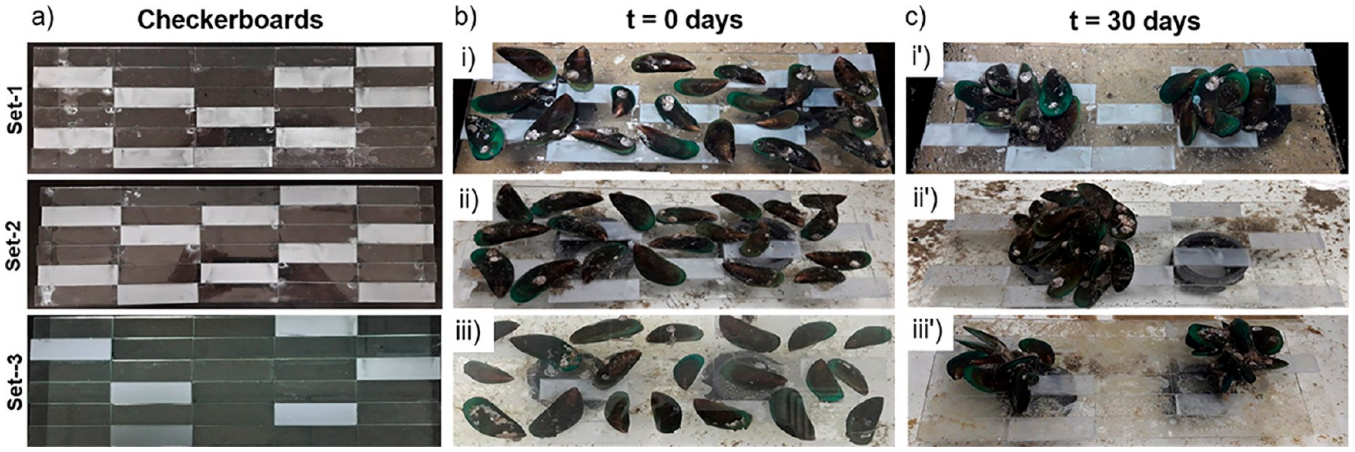

Figure 4. Assessment of the fouling prevention capacity of SLIPS coatings using a mussel settlement assay on randomized multiple-coating checkerboards. SM, SC, and SN-coated slides were randomly arranged in a checkerboard panel and 20 mussels were regularly placed on the checkerboard and allowed to explore the surface for 30 days. (a) Three independent checkerboards illustrating the randomized checkerboard arrangement of the various surfaces. Both sets 1 and 2 contained 3 different SLIPS-coated slides (SM, SC, and SN; 10 slides each), whereas set 3 contained the 3 SLIPS-coated slides plus 2 additional types of coated slides (iPDMS and PDMS; 6 slides each). (b) Pictures of the checkerboard at t = 0 day illustrating the regular arrangement of mussels. (c) Pictures of the checkerboard showing mussel settlement after t = 30 days (i′−iii′). Following the settlement assay, each coated slide was visually inspected, and the number of adhesive plaques counted as presented in Figure 5.

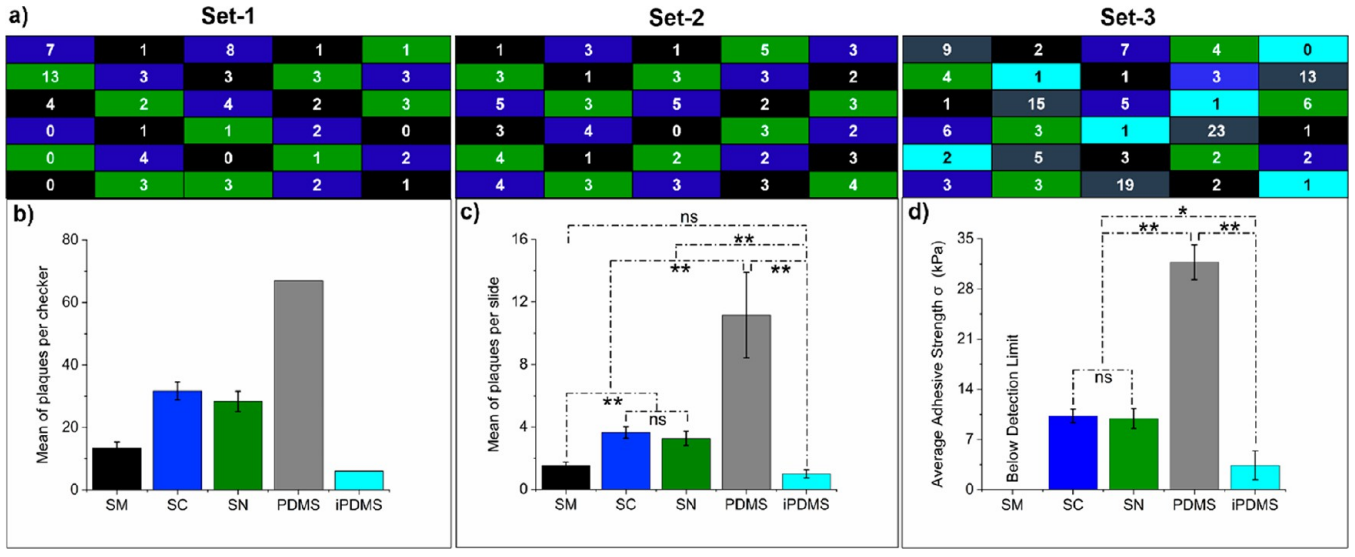

Figure 5. (a) Quantitative results of checkerboard multiple choice assay. The number on each slide corresponds to the number of adhesive plaques counted after one month of testing. Surface color codes: SM (black), SC (blue), SN (green), PDMS (grey), iPDMS (cyan). (b) Mean number of plaques per checker. (c) Mean number of plaques per slide. (d) Average adhesive strength on the different surfaces. Differences between average values in panels c and d indicated with asterisks are statistically significant for the null-hypothesis given by the t-test, in which * and ** illustrate $p < 0.05$ and $p < 0.001$ respectively. ns: Statistically nonsignificant.

the mussel foot (Figure 5a−c). After immersion for a few months in seawater, capillary adhesive forces ($F^{\$}$) between SN, SC, and SM surfaces did not change significantly (Figure 3e and f, Table 2). However, the capillary bridge height of SM ($H^{\$}_{SM}$) was significantly affected and reduced almost 4-fold compared to the fresh sample (Table 2 and Figure 3e and f). This reduction of capillary length suggests a faster depletion rate of the lubricant, which could affect the fouling-resistance efficacy of SM over longer periods of times. In contrast, lubricant leakage was not as pronounced for SC and

https://dx.doi.org/10.1021/acsapm.0c00916
ACS Appl. Polym. Mater. 2020, 2, 5147−5162

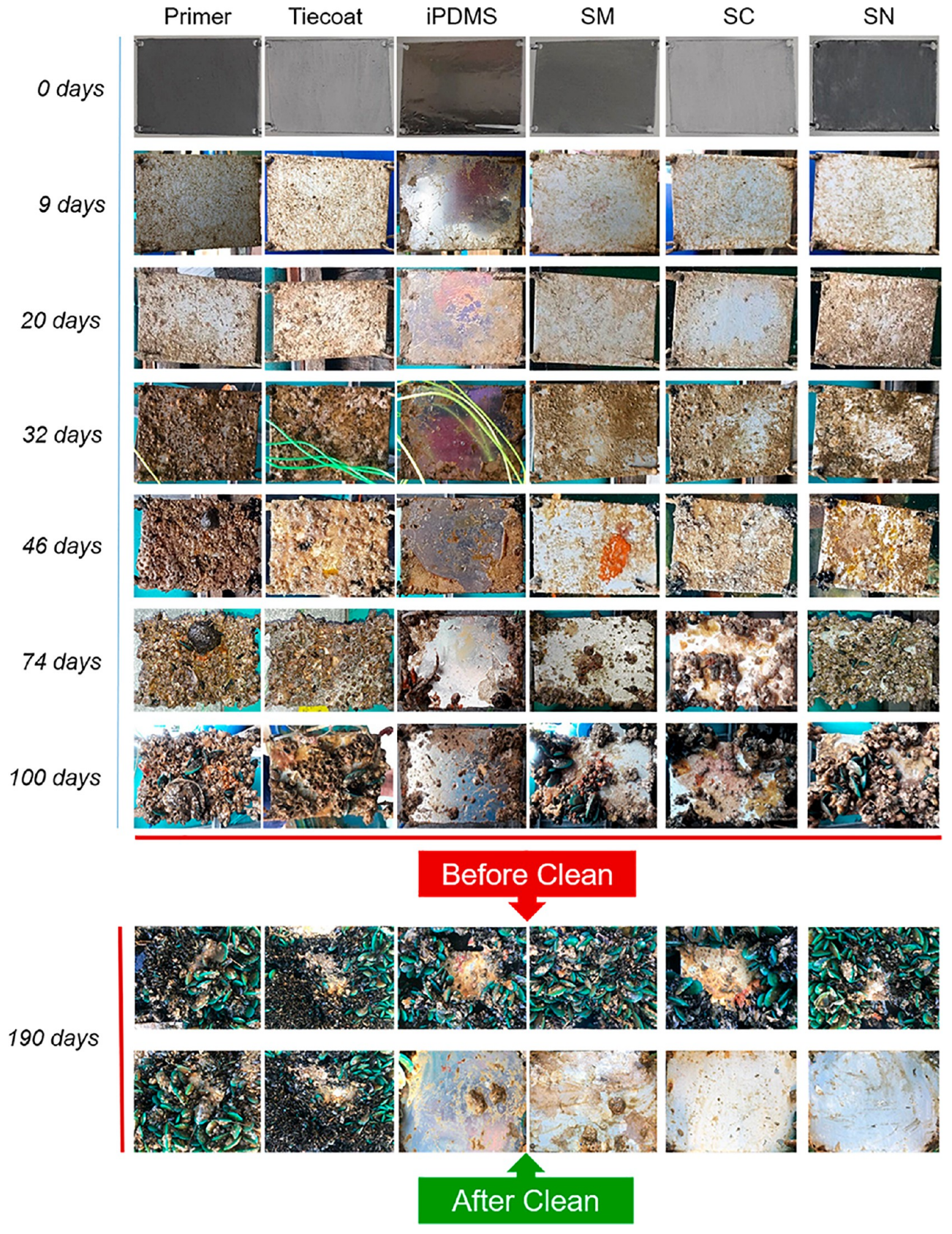

Figure 6. Biofouling results of the field study carried out in stagnant water conditions in a mussel aquaculture farm. Three coatings (SM, SC, and SN) were evaluated as well as three control samples (Primer 300, Tie-coat 731, iPDMS) for 190 days.

SN samples, and these coatings also contain a reduced amount of lubricant in their formulation. In agreement with partial depletion of the lubricant phase, the modulus of all coatings slightly increased after immersion in seawater for five

https://dx.doi.org/10.1021/acsapm.0c00916
ACS Appl. Polym. Mater. 2020, 2, 5147−5162

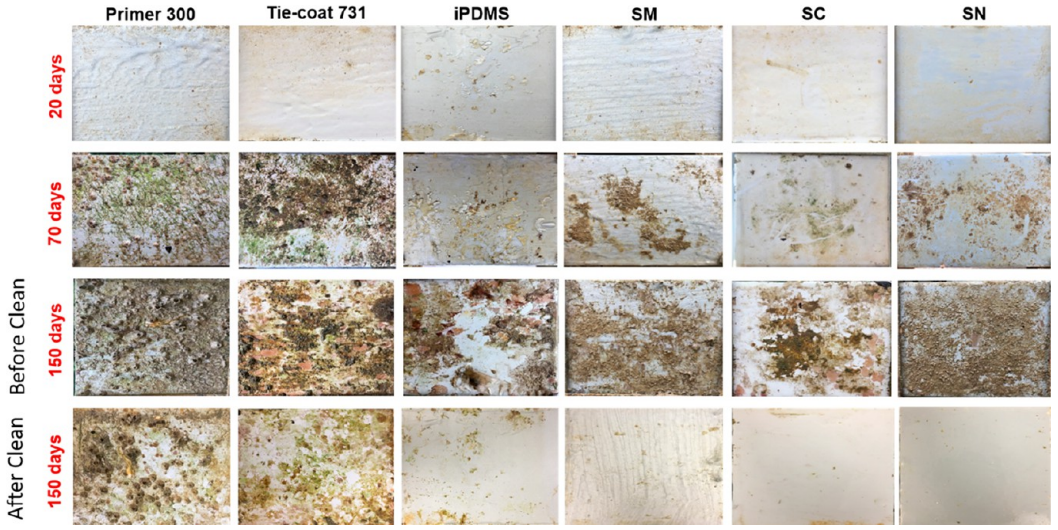

Figure 7. Biofouling results of the field study carried out under strong hydrodynamic currents. Three coatings (SM, SC, and SN) were evaluated as well as three control samples (Primer 300, Tie-coat 731, iPDMS) for 150 days.

months (Figure 3b, Table 2), as would be expected if swelling of the coating network decreases due a lower fraction of lubricant in the network.

Mussel Multichoice Settlement Assay. To assess the fouling resistance of the coatings in the lab, we used green mussels as a model species. Green mussels are highly abundant along the shores of the tropical Indo-Pacific and are very efficient at fouling a wide range of solid surfaces.[49] We used a checkerboard design as described elsewhere[28,39] consisting in randomly fixing glass slides coated with the different coatings on the checkerboard, placing mussels on top of the board, and letting them explore all surfaces for 1 month under artificial seawater conditions (Figure 4a and b). For one checkerboard, in addition to the three commercial coating samples, PDMS and iPDMS were also tested as control substrates. For the two remaining checkerboards, only the commercial coatings were tested in order to obtain a direct comparison between these coatings and avoid bias toward the control substrate (PDMS) known to "attract" more mussels. At the end of the assay, mussels mainly aggregated into 1 or 2 clusters on all three checkerboards (Figure 4c). Visual inspection of the checkerboard comprising the control PDMS and iPDMS confirmed the larger number of plaques on PDMS compared to all other slippery coatings (Figure S4). The number of plaques per checkerboard on PDMS was 85 versus 32 for SC, 28 for SN, and 13 for SM, while iPDMS contained only a handful of plaques (Figure 5a and b). We note that the hydrophilic SN coating contained a similar number of adhesive plaques as the hydrophobic SC coating, whereas the second hydrophobic coating (SM) contained 2 fold fewer plaques and the results were statistically significant in terms of mean number of plaques per checkerboard and mean number of plaques per slide (Figure 5c) These results indicate that the hydrophobic/hydrophilic nature of the slippery coatings has little influence on the settlement preference of mussels and that the ability of a slippery coating to prevent plaque deposition is governed by different parameters. In our previous study on iPDMS,[28] we proposed that the lubricant overlayer shields the underlying solid coating from being detected by the mussel foot (the organ used to probe and secrete threads), in turn disrupting thread secretion. Accordingly, a thicker lubricant layer is expected to be more efficient at masking the substrate from the mussels. This is consistent with the capillary bridge results (Figure 3), which show that the initial capillary bridge length of SM (containing a higher volume fraction of lubricant) is ~30 μm, about 3-fold larger than SC and SN (~10 μm).

Plaques Adhesive Strength. To evaluate the FR efficiency of the coatings, we measured the adhesion strength (σ_{ad}) of individual mussel adhesive filaments using a customized micromechanical equipment (see Materials and Methods), since this property should provide a direct proxy for the ease of mussel removal in practical situations. The average σ_{ad} values for SC (hydrophobic) and SN (hydrophilic) coatings (Figure 5d) were not statistically different (10.3 ± 0.95 and 9.9 ± 1.4 kPa, respectively) and ~3-fold lower than PDMS (30.3 ± 6.7 kPa). Although the adhesion was not as weak as for the lab-scale iPDMS coating (3.4 ± 2.0 kPa),[28] these results nevertheless indicate that foul-release would be greatly facilitated on these coatings compared to PDMS (which is already considered an efficient FR material)[50] as verified in our field studies described in the next section. The hydrophobic SM coating performed even better, with an adhesion strength that was below the detection limit of the force sensor (<2 kPa). It is noteworthy that the "adhesive performance index" (where coatings that perform best in terms of foul-release efficiency have the lowest σ_{ad} values) exhibited the same trend as the checkerboard assay; namely, the SM coating was the best performer, whereas SC and SN coatings were not statistically different. This correlation is in agreement with the notion that inhibition of settlement and weak adhesion of mussels on slippery coatings are both linked to the presence of the lubricant film. As detailed in Amini et al. (2017),[28] the film lowers the thermodynamic work of adhesion (w_a) of adhesive plaques and also affects the effective area of a plaque in contact with the substrate, which in turn decrease the macroscopic adhesion strength σ_{ad}. A thicker lubricant film on the surface of the coating is thus anticipated to lower σ_{ad} just like it is more efficient at shielding the substrate from the mussels, and these correlations would remain valid as long as

https://dx.doi.org/10.1021/acsapm.0c00916
ACS Appl. Polym. Mater. 2020, 2, 5147−5162

the thickness of the lubricant overlayer remains unchanged. However, nanomechanical measurements after a few months of immersion in the field indicated some depletion of lubricant over time (Figure 3), which could affect the long-term performance of the coatings. To answer this question, field testing experiments were performed.

Fouling-Resistance of the Coatings in the Field. Field studies were conducted both under stagnant water and strong hydrodynamic forces conditions created by tidal currents (see Materials and Methods for more details). Under stagnant water conditions, all commercial coatings as well as the three control coatings (primer, tie-coat, and iPDMS) were immersed (Figure S1b) and visually inspected at different time intervals during more than 6 months (190 d), after which the panels were cleaned to assess the ease of fouling removal. In addition, biofilms were also collected at the sixth and fifth month from Lorong Halus (Figure 6) and Sentosa (Figure 7), respectively from all coatings in order to assess the bacterial biofilm composition using 16S amplicon metagenomic sequencing.

For the site where water was relatively stagnant, in the first 20 d all coatings showed little macrofouling and were mostly colonized by microbial biofilms (Figure 6). Metagenomics showed that bacteria were present on all coatings. Up to 50 bacterial families were detected and the most abundant bacterial family in the Lorong Halus site was *Rhodobacteraceae* (Figure S5). The other bacterial species detected were typical members of a marine biofilm community like the *Halieaceae* and *Vibrionaceae*. Five bacterial families (*Alteromonadaceae, Kordiimonadaceae, Lentisphaeraceae, Desulfarculaceae, Alcanivoracaceae*) were absent on the SC surfaces, but these made up a very small percentage of the total abundance on other surfaces deployed at Lorong Halus (between 0.04% and 4.68%). When all the samples were considered, principle covariate analysis using UniFrac distances showed that the replicates within sampling sites were relatively well grouped. The main differences in bacterial community compositions were observed between the testing sites (Figure S5). However, when the communities in the Lorong Halus site were tested for differences based on whether the coatings were hydrophobic or hydrophilic, statistical analysis indicated a slight difference with a *p*-value of 0.0991 (Figure 8).

On the control surfaces (primer and tie-coat), significant coverage of barnacles was observed at 32 d and their incrustation then rapidly increased over time. Mussels started to appear at 100 d and then fully covered the plates. On hydrophobic (SM and SC) slippery coatings, barnacles first fouled the SC coating (at 32 d) and appeared later on the SM coating (74 d). Mussels were observed at 100 d, mostly on the edge of the panels. On the hydrophilic SN coating, barnacles and mussels concurrently appeared at 74 d and then steadily increased. After 190 d, the supporting frame was fully covered with macrofoulers, notably because mussels could readily settle from the noncoated edges and the attachment strings of the frame (Figure S1c), and members of the colony subsequently attached to the first settlers. However, the fouling-release performance—as evaluated by the ease of detachment of mussel beds—was radically different between the control and the slippery coatings, as illustrated in Movies S1–S6. Although not quantitative, the method gave a qualitative assessment of external forces required to remove the foulers from the surface. On the control samples (primer and tie-coat), detachment was

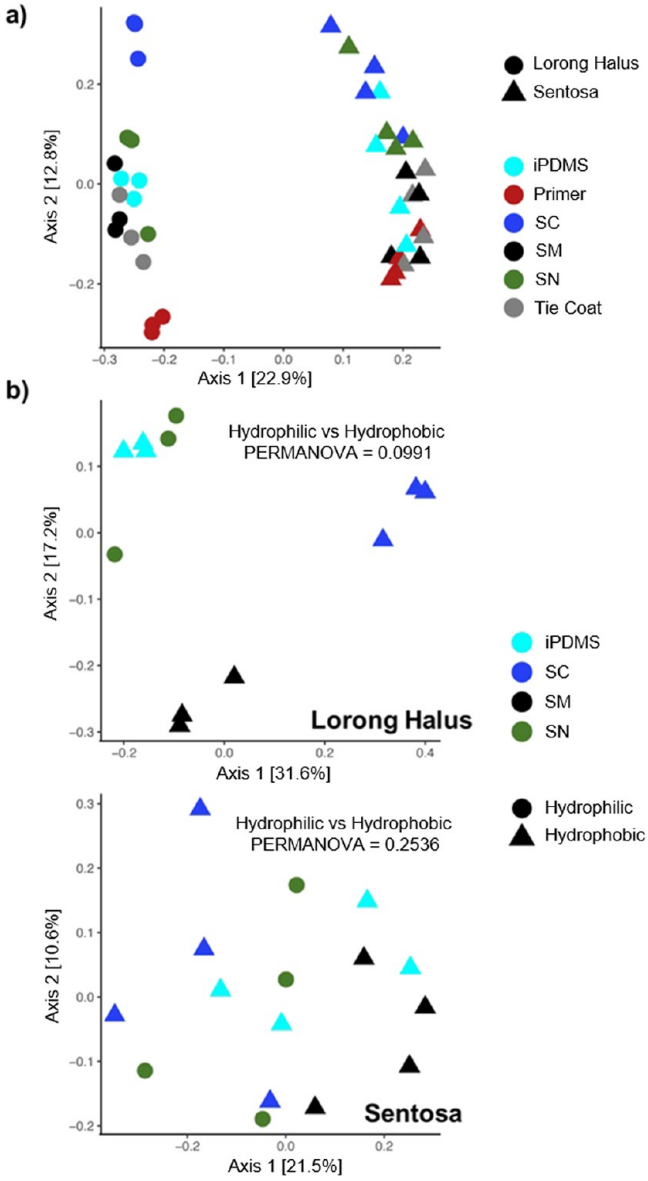

Figure 8. (a) Principle coordinate analysis of the samples distance matrix. The distance matrix was calculated using unweighted UniFrac distance. The sampling site is indicated by shape and the type of coatings are differentiated by color. (b) Principle coordinate analysis of the coatings separated by sampling site and the distance matrices calculated using unweighted UniFrac distance. The coatings are indicated by color while the characteristic is differentiated by shape. The PERMANOVA analysis was done to test for differences between the hydrophilic and hydrophobic coatings using the adonis function in the vegan v 2.5–6 package with 9999 permutations.

exceedingly difficult as macrofoulers were firmly incrusted on the samples: manual removal was not possible in these cases (Movies S1 and S2). In stark contrast, removal of mussel from the slippery coatings was much smoother, requiring just moderate forces to peel off the entire bed of mussels (Movies S3–S6). We could not perceive differences in the ease of release between the different coatings. Overall, the facile detachment of macrofoulers from the panels suggest that mussels found in the immediate proximity of the slippery coatings secreted their byssal threads around the substrates and on the edge of the frame but largely avoided direct deposition of adhesive plaques on the coatings. Subsequently,

https://dx.doi.org/10.1021/acsapm.0c00916
ACS Appl. Polym. Mater. 2020, 2, 5147–5162

new mussels attached onto the shells of the first layer of mussels. As a result, mussel colonies could be readily detached because there were only a few threads that were directed secreted on the coated surfaces. In the case of attachment, only moderate force was required to detach the mussel colony, in agreement with the low adhesion strength measured for individual adhesive filaments (Figure 5d).

Fouling results on coatings immersed under stronger hydrodynamic conditions (see Figure S2 for a picture of the frame and the location of the experiments) are presented in Figure 7. After 20 d, thin biofilms were observed on all samples (Figure 7) with no visible significant differences between the coatings. Similar to the Lorong Halus samples, bacterial families were detected on all coatings. However, the most abundant bacterial family was *Sphingomonadaceae*, followed by *Rhodobacteraceae* and SS1-B-06-26. The members of the community are typical members of a marine bacteria, and their relative abundances were not statistically different between the coatings. Likewise, the replicates within the sites were also well-grouped and the different sites overlapped, suggesting high similarities between the bacterial communities on the different coatings.

After 70 d, coverage of soft foulers was much more visible on the control samples, which were later fouled by barnacles (150 d onward). On all slippery coatings, the coverage and mass of biofilm steadily increased with no significant differences between the coatings, but hard foulers were not detected after 150 d of immersion. Similar to the panels immersed in stagnant water conditions, the control samples were heavily incrusted by the fouling organisms and could not be manually cleaned Movies S7 and S8). In contrast, a smooth rub could easily remove the biofilms from all slippery coatings (Movies S9−S12).

DISCUSSION

FR coatings that can efficiently thwart marine biofouling have been a central focus of research and development efforts of antifouling technologies in the past decade,[22,51] both by the academic community and commercial companies. Slippery coatings[45,52] have shown potential to combat marine biofouling in the laboratory and on small scale samples.[27,28,39,53] Commercial coatings exploiting this technology for large-scale applications are currently being developed and this study provides a first assessment of their fouling-resistance capacities, both in the lab as well as in environmental conditions subjected to heavy fouling stresses.

While there is no "universal" mechanism of marine biofouling, it is generally accepted that colonization starts with the adsorption of an organic matter conditioning film as soon as surfaces are immersed,[1,23] usually followed by the secretion of bacteria-induced biofilms whose initial adhesion is influenced by the surface energy of the substrate.[54,55] It is known that colonization of macrofoulers are affected by chemical cues[56] and that biofilms are key mediators in this process. While detailed studies of chemical cues by a system like biofilms and their effects on macrofouler colonization are limited,[57] there are studies that positively correlate macrofouler settlement to acyl-homoserine lactones (AHL).[58,59] Although AHLs are produced by several microbes, the chemical profiles are likely to vary qualitatively and quantitatively.[60] Therefore, having similar bacteria composition on the different coatings suggests that any differences in efficiency of antifouling would not be due to the preference of macrofoulers for surfaces precolonized by certain bacteria that released certain cues but instead related to the intrinsic physicochemical properties of the coatings.

Both environmental factors (salinity, pH, temperature, nutrient levels, flow rates, and the intensity of solar radiation) and material properties influence the subsequent settlement of marine foulers.[61,62] The surface energy of the substrate is generally viewed as playing an important role during the settlement of marine biofoulers on sea-immersed surfaces, but surface energy considerations alone are not sufficient to explain the settlement preference of macrofoulers.[63] For example, adult barnacles prefer to settle on high surface energy content surface (30−35 mN/m),[64] whereas barnacle cyprids do not appear to show a preference for either high- or low-energy surface coatings.[65] Mussels can efficiently attach to both hydrophobic and hydrophilic surfaces[66,67] through their multiprotein byssal filaments;[68,69] however, SLIPS-based surfaces can largely disrupt the secretion process, as well as minimize the adhesion strength of the byssal filaments as corroborated in our lab-scale measurements. Instead, the lubricant overlayer is the key design element providing fouling-resistance in this case and should in principle work independently on whether the underlying surface is hydrophobic or hydrophilic. This hypothesis is supported in this study as no significant differences in settlement and adhesion strength were observed between hydrophobic (SC) and hydrophilic (SN) coatings. A more important criterion appears to be the thickness of the lubricant trapped in the coating that forms an overlayer slippery film on the surface, and the initial film thickness could be quantified using contact mechanics measurements in terms of capillary bridge length (Figure 3). The SM coating formulation contains a higher relative amount of lubricant, resulting in a longer capillary bridge layer (~30 μm vs 12−20 μm for SN and SC coating) as well as a lower elastic modulus due to enhanced swelling, and this coating exhibited lower mussel settlement and weaker adhesion strength (<2 kPa, which is the detection limit of our custom-made microtensile tester). Yet, the larger lubricant content also leads to its faster depletion rate after multimonths exposure in the field, as indicated by the reduced capillary bridge length (Figure 3f) and by the increase in elastic modulus, which is attributed to lower swelling of the network as the lubricant content decays (it is also worth noting that these two properties, here measured by depth-sensing nanoindentation, provide quantitative information on the aging of slippery coatings). Thus, overtime the benefit of a higher lubricant volume may no longer be obvious.

Field studies under stagnant waters in an extreme fouling stress environment (a mussel aquaculture farm) showed that hard macrofoulers were observed over the coatings after 3−4 months of immersion but that fouling largely initiated from the (uncoated) edge and attachment fixtures of the fouling frame. There was minimal direct settlement onto the coatings themselves and the fouling colonies could easily be detached on all slippery coatings with no significant difference depending on the surface energy. After a long exposure time, the high volume of lubricant did not appear to enhance the fouling resistance and all coatings displayed almost equal fouling release performance. Moreover, 1−2 barnacles were attached on the SM and iPDMS samples and were difficult to remove by applying moderate forces. For panels subjected to strong current conditions chosen to simulate the hydro-

https://dx.doi.org/10.1021/acsapm.0c00916
ACS Appl. Polym. Mater. 2020, 2, 5147−5162

dynamic conditions of a moving vessel, only biofilms were found on the surfaces of the coated samples after 5 months of immersion. These biofilms could be readily removed from the surface. Practically, this implies that hull maintenance could be carried out with a minimum water jet pressure.

Hydrophilic slippery surfaces (here, SN) offer the option to provide fouling protection against different types of fouling organisms, such as green algae, diatoms or bacteria that are less efficient at fouling amphiphilic surfaces.[1,23,24] It may also help in minimizing adsorption of the conditioning film, since most proteins (the major component of the conditioning film) that contaminate solid surfaces are hydrophobic in nature and the hydration layer formed on the hydrophilic polymer prevents proteins adhesion to the infused surface.[70] On the basis of our results, this coating is anticipated to perform well in environments with low fouling stresses, but may not be advantageous in conditions of high fouling stresses (in particular macrofoulers) since these organisms do not demonstrate obvious fouling preference for a certain type of surface energy,[22,65] especially for slippery surfaces as confirmed in this study. Ultimately, the intended application and the local conditions of the fouling environment (diversity and density of fouling species, hydrodynamic flow, temperature, salinity, etc.) will dictate the preferred choice of coatings.

CONCLUSIONS

Slippery coatings exhibit promising fouling-resistant properties in a wide range of fouling environments, including marine ecosystems. In this study, the fouling-resistance of commercial slippery coatings was evaluated both in lab and field studies. The coatings were silicon-based with various relative amount of entrapped lubricants, and both hydrophobic and hydrophilic formulations were investigated. In the lab, using the Asian green mussel as a model macrofouling organism, all coatings prevented significant mussel settlement. The best performing coating—defined by the ability to inhibit secretion of adhesive plaques and by a weak interfacial adhesive strength—contained a higher volume of lubricant. At similar lubricant content, there were no significant differences between hydrophobic and hydrophilic coatings. In field studies performed in the tropical, high-fouling water environment of Singapore, no obvious differences were observed between the different types of coatings, which all performed equivalently against marine biofouling: in stagnant waters of an aquaculture farm, macrofouling organisms were readily detached from all coatings, whereas in high current water conditions only biofilms weakly attached to the surfaces and these biofilms could be removed with moderate shearing forces. The slippery coatings, including preconditioned hydrophilic SN containing an amphiphilic polymer, did not display cytotoxicity against a fish gill cell line used as a proxy to assess the potential toxicity of the coatings. Thus, while slippery coatings with a higher lubricant volume performs better in the short term and in the lab, this advantage is no longer apparent over multimonth of immersion in the field. Suitable characteristics to assess aging of slippery coatings are the surface elastic modulus and the length of a capillary bridge at the lubricant/water interface—both of which can be accurately measured by depth-sensing nanoindentation—since these properties are directly linked to the amount of entrapped lubricant remaining in the coating. Finally, it is often considered that low surface energy coatings have superior antifouling ability. The present study indicates that high surface energy (hydrophilic), slippery coatings can resist equally well against marine biofouling, providing new insights to fabricate effective antifouling surfaces.

ASSOCIATED CONTENT

Supporting Information

The Supporting Information is available free of charge at https://pubs.acs.org/doi/10.1021/acsapm.0c00916.

Design and installation of the SLIPS samples in the seawater at Lorong Halus, Singapore; design and installation of the SLIPS samples at Sentosa, Singapore; CA measurements on coatings kept in air for 1 year and immersed in seawater for 5 months; adhesives plaques on infused surfaces after 1 month of the multiple choice assay; and bacterial community compositions assessed by metagenomics sequencing (PDF)

Movie S1: Marine biofoulers' adhesion and detachment from the SLIPS (SN, SM, SC) and control (Primer 300 and Tie-coat 731) surfaces immersed at an aquaculture farm in Lorong Halus (MOV)

Movie S2: Marine biofoulers' adhesion and detachment from the SLIPS (SN, SM, SC) and control (Primer 300 and Tie-coat 731) surfaces immersed at an aquaculture farm in Lorong Halus (MOV)

Movie S3: Marine biofoulers' adhesion and detachment from the SLIPS (SN, SM, SC) and control (Primer 300 and Tie-coat 731) surfaces immersed at an aquaculture farm in Lorong Halus (MOV)

Movie S4: Marine biofoulers' adhesion and detachment from the SLIPS (SN, SM, SC) and control (Primer 300 and Tie-coat 731) surfaces immersed at an aquaculture farm in Lorong Halus (MOV)

Movie S5: Marine biofoulers' adhesion and detachment from the SLIPS (SN, SM, SC) and control (Primer 300 and Tie-coat 731) surfaces immersed at an aquaculture farm in Lorong Halus (MOV)

Movie S6: Marine biofoulers' adhesion and detachment from the SLIPS (SN, SM, SC) and control (Primer 300 and Tie-coat 731) surfaces immersed at an aquaculture farm in Lorong Halus (MOV)

Movie S7: Marine biofoulers' adhesion and detachment from the SLIPS (SN, SM, SC) and control (Primer 300 and Tie-coat 731) surfaces immersed at Sentosa boardwalk (AVI)

Movie S8: Marine biofoulers' adhesion and detachment from the SLIPS (SN, SM, SC) and control (Primer 300 and Tie-coat 731) surfaces immersed at Sentosa boardwalk (AVI)

Movie S9: Marine biofoulers' adhesion and detachment from the SLIPS (SN, SM, SC) and control (Primer 300 and Tie-coat 731) surfaces immersed at Sentosa boardwalk (AVI)

Movie S10: Marine biofoulers' adhesion and detachment from the SLIPS (SN, SM, SC) and control (Primer 300 and Tie-coat 731) surfaces immersed at Sentosa boardwalk (AVI)

Movie S11: Marine biofoulers' adhesion and detachment from the SLIPS (SN, SM, SC) and control (Primer 300 and Tie-coat 731) surfaces immersed at Sentosa boardwalk (AVI)

https://dx.doi.org/10.1021/acsapm.0c00916
ACS Appl. Polym. Mater. 2020, 2, 5147−5162

Movie S12: Marine biofoulers' adhesion and detachment from the SLIPS (SN, SM, SC) and control (Primer 300 and Tie-coat 731) surfaces immersed at Sentosa boardwalk (AVI)

AUTHOR INFORMATION

Corresponding Author

Ali Miserez − *Centre for Biomimetic Sensor Science (CBSS), School of Materials Science and Engineering, Nanyang Technological University (NTU), Singapore 63 9798, Singapore; School of Biological Sciences, NTU, Singapore 63 7551, Singapore;* orcid.org/0000-0003-0864-8170; Email: ali.miserez@ntu.edu.sg

Authors

Snehasish Basu − *Centre for Biomimetic Sensor Science (CBSS), School of Materials Science and Engineering, Nanyang Technological University (NTU), Singapore 63 9798, Singapore*

Bui My Hanh − *Centre for Biomimetic Sensor Science (CBSS), School of Materials Science and Engineering, Nanyang Technological University (NTU), Singapore 63 9798, Singapore*

Muhammad Hafiz Ismail − *Singapore Centre for Environmental Life Sciences Engineering (SCELSE), NTU, Singapore 63 7551, Singapore;* orcid.org/0000-0002-2890-0444

J. Q. Isaiah Chua − *Centre for Biomimetic Sensor Science (CBSS), School of Materials Science and Engineering, Nanyang Technological University (NTU), Singapore 63 9798, Singapore*

Srikanth Narasimalu − *Energy Research Institute at NTU (ERI@N), Singapore 63 7141, Singapore*

Manoj Sekar − *Energy Research Institute at NTU (ERI@N), Singapore 63 7141, Singapore*

Andrew Labak − *Adaptive Surface Technology, Inc., Cambridge, Massachusetts 0214, United States*

Alex Vena − *Adaptive Surface Technology, Inc., Cambridge, Massachusetts 0214, United States*

Philseok Kim − *Adaptive Surface Technology, Inc., Cambridge, Massachusetts 0214, United States*

Teluka P. Galhenage − *Adaptive Surface Technology, Inc., Cambridge, Massachusetts 0214, United States*

Scott A. Rice − *Singapore Centre for Environmental Life Sciences Engineering (SCELSE), NTU, Singapore 63 7551, Singapore; School of Biological Sciences, NTU, Singapore 63 7551, Singapore;* orcid.org/0000-0002-9486-2343

Complete contact information is available at: https://pubs.acs.org/10.1021/acsapm.0c00916

Author Contributions

S.B. designed and conducted experiments (biofouling testing, surface characterization, nanomechanics), analyzed data, and wrote the manuscript. B.M.H. conducted biofouling testing and adhesion strength experiments and analyzed data. M.H.I. conducted and analyzed cytotoxicity and metagenomic experiments and wrote the associated content. J.Q.I.C. advised and helped with contact nanomechanics experiments. S.N. designed a testing metallic frame for biofouling experiments at Sentosa boardwalk and helped provide a site for testing. M.S. designed and built metallic frame for biofouling testing. A.L. and A.V. prepared commercial coatings and advised on coating preparation. P.K. designed commercial coatings, advised on biofouling testing, and managed the NTU/AST collaboration. T.P.G. designed commercial coatings, advised on field-assay biofouling testing, managed NTU/AST collaboration, and provided editorial comments. S.A.R. designed and supervised metagenomic experiments and provided editorial comments on the manuscript. A.M. designed and supervised the overall study, analyzed data, and wrote the manuscript.

Notes

The authors declare the following competing financial interest(s): Adaptive Surface Technologies, Inc. (authors A.L, A.V, P.K, and T.P.K.), provided the coatings investigated in this study.

ACKNOWLEDGMENTS

This study was funded by the Singapore National Research Foundation under its Marine Science Research and Development Program (MSRDP), Grant MSRDP-P29. Financial support was also provided from the Singapore Centre for Environmental Life Sciences Engineering (SCELSE), whose research is supported by the National Research Foundation Singapore and Ministry of Education under its Research Centre of Excellence Programme. We thank W. Kai for providing access to his aquaculture farm and for regularly checking the structural condition of the testing frame.

REFERENCES

(1) Callow, J. A.; Callow, M. E. Trends in the Development of Environmentally Friendly Fouling-resistant Marine Coatings. *Nat. Commun.* **2011**, *2*, 244.

(2) Dürr, S., Thomason, J., Eds. *Biofouling*, 1st ed.; Wiley-Blackwell: Chichester, West Sussex, England, 2010.

(3) Schultz, M. P.; Bendick, J. A.; Holm, E. R.; Hertel, W. M. Economic impact of biofouling on a naval surface ship. *Biofouling* **2011**, *27*, 87−98.

(4) Poloczanska, E. S.; Babcock, R. C.; Butler, A.; Hobday, A.; HoeghGuldberg, O.; Kunz, T. J.; Matear, R.; Milton, D. A.; Okey, T. A.; Richardson, A. J. Climate change and Australian marine life. *Oceanogr. Mar. Biol.* **2007**, *45*, 407−478.

(5) Page, H. M.; Hubbard, D. M. Temporal and spatial patterns of growth in mussels Mytilus edulis on an offshore platform: relationships to water temperature and food availability. *J. Exp. Mar. Biol. Ecol.* **1987**, *111*, 159−179.

(6) Valdez, B.; Ramirez, J.; Eliezer, A.; Schorr, M.; Ramos, R.; Salinas, R. Corrosion assessment of infrastructure assets in coastal seas. *J. Mar. Eng. Technol.* **2016**, *15*, 124−134.

(7) Coetser, S. E.; Cloete, T. E. Biofouling and biocorrosion in industrial water systems. *Crit. Rev. Microbiol.* **2005**, *31*, 213−232.

(8) Dexter, S. C. Role of microfouling organisms in marine corrosion. *Biofouling* **1993**, *7*, 97−127.

(9) Rajagopal, S.; Venugopalan, V. P.; van der Velde, G.; Jenner, H. A. Greening of the coasts: a review of Perna viridis success story. *Aquat. Ecol.* **2006**, *40*, 273−297.

(10) Strayer, D. L. Twenty years of zebra mussels: Lessons from the mollusk that made headlines. *Front. Ecol. Environ.* **2009**, *7*, 135−141.

(11) Gantayet, A.; Ohana, L.; Sone, E. D. Byssal proteins of the freshwater zebra mussel, Dreissena polymorpha. *Biofouling* **2013**, *29*, 77−85.

(12) Alzieu, C. Tributyltin: case study of a chronic contaminant in the coastal environment. *Ocean Coast Manage.* **1998**, *40*, 23−26.

(13) Nehring, S. A. After the TBT era: Alternative anti-fouling paints and their ecological risks. *Senckenbergiana Marit.* **2001**, *31*, 341−351.

(14) Pereira, M.; Ankjaergaard, C. In *Advances in Marine Antifouling Coatings and Technologies*; Woodshead Publishing: Cambridge, U.K., 2009; p 240.
(15) Ytreberg, E.; Karlsson, J.; Eklund, B. Comparison of toxicity and release rates of Cu and Zn from anti-fouling paints leached in natural and artificial brackish seawater. *Sci. Total Environ.* **2010**, *408*, 2459−2466.
(16) Olsen, S. M.; Pedersen, L. T.; Laursen, M. H.; Kiil, S.; Dam-Johansen, K. Enzyme-based antifouling coatings: a review. *Biofouling* **2007**, *23*, 369−383.
(17) Al-Juhni, A. A.; Newby, B.-M. Z. Incorporation of benzoic acid and sodium benzoate into silicone coatings and subsequent leaching of the compound from the incorporated coatings. *Prog. Org. Coat.* **2006**, *56*, 135.
(18) Soethe, V. L.; Delatorre, R. G.; Ramos, E. M.; Parucker, M. L. TiO_2 thin Films for Biofouling Applications. *Mater. Res.* **2017**, *20*, 426−31.
(19) Bullock, S.; Johnston, E. E.; Willson, T.; Gatenholm, P.; Wynne, K. J. Surface Science of a Filled Polydimethylsiloxane-Based Alkoxysilane-Cured Elastomer: RTV11. *J. Colloid Interface Sci.* **1999**, *210*, 18.
(20) Xue, C.-H.; Jia, S.-T.; Zhang, J.; Tian, L. Q.; Chen, H. Z.; Wang, M. Preparation of superhydrophobic surfaces on cotton textiles. *Sci. Technol. Adv. Mater.* **2008**, *9*, No. 035008.
(21) Ou, L.; Song, B.; Liang, H.; Liu, J.; Feng, X.; Deng, B.; Sun, T.; Shao, L. Toxicity of graphene-family nanoparticles: a general review of the origins and mechanisms. *Part. Fibre Toxicol.* **2016**, *13*, 57.
(22) Lejars, M.; Margaillan, A.; Bressy, C. Fouling Release Coatings: A Nontoxic Alternative to Biocidal Antifouling Coatings. *Chem. Rev.* **2012**, *112*, 4347−4390.
(23) Peppou-Chapman, S.; Hong, J. K.; Waterhouse, A.; Neto, C. Life and death of liquid-infused surfaces: a review on the choice, analysis and fate of the infused liquid layer. *Chem. Soc. Rev.* **2020**, *49*, 3688−3715.
(24) Galhenage, T. P.; Webster, D. C.; Moreira, A. M. S.; Burgett, R. J.; Stafslien, S. J.; Vanderwal, L.; Finlay, J. A.; Franco, S. C.; Clare, A. S. Poly(ethylene) glycol-modified, amphiphilic, siloxane-polyurethane coatings and their performance as fouling-release surfaces. *J. Coat. Technol. Res.* **2017**, *14*, 307−322.
(25) Beigbeder, A.; Linares, M.; Devalckenaere, M.; Degee, P.; Claes, M.; Beljonne, D.; Lazzaroni, R.; Dubois, P. CH-π Interactions as the Driving Force for Silicone-Based Nanocomposites with Exceptional Properties. *Adv. Mater.* **2008**, *20*, 1003.
(26) Jiang, S. Y.; Cao, Z. Q. Ultralow-Fouling, Functionalizable, and Hydrolyzable Zwitterionic Materials and Their Derivatives for Biological Applications. *Adv. Mater.* **2010**, *22*, 920−932.
(27) Xiao, L.; Li, J.; Mieszkin, S.; Di Fino, A.; Clare, A. S.; Callow, M. E.; Callow, J. A.; Grunze, M.; Rosenhahn, A.; Levkin, P. A. Slippery Liquid-Infused Porous Surfaces Showing Marine Antibiofouling Properties. *ACS Appl. Mater. Interfaces* **2013**, *5*, 10074−10080.
(28) Amini, S.; Kolle, S.; Petrone, L.; Ahanotu, O.; Sunny, S.; Sutanto, C. N.; Hoon, S.; Cohen, L.; Weaver, J. C.; Aizenberg, J.; Vogel, N.; Miserez, A. Preventing mussel adhesion using lubricant-infused materials. *Science* **2017**, *357*, 668.
(29) MacCallum, N.; Howell, C.; Kim, P.; Sun, D.; Friedlander, R.; Ranisau, J.; Ahanotu, O.; Lin, J. J.; Vena, A.; Hatton, B.; Wong, T.-S.; Aizenberg, J. Liquid Infused Silicone as a Biofouling-Free Medical Material. *ACS Biomater. Sci. Eng.* **2015**, *1*, 43−51.
(30) Cui, J. X.; Daniel, D.; Grinthal, A.; Lin, K. X.; Aizenberg, J. Dynamic polymer systems with self-regulated secretion for the control of surface properties and material healing. *Nat. Mater.* **2015**, *14*, 790−795.
(31) Cao, S.; Wang, J. D.; Chen, H. S.; Chen, D. R. Progress of marine biofouling and antifouling technologies. *Chin. Sci. Bull.* **2011**, *56*, 598−612.
(32) Swain, G. W.; Anil, A. C.; Baier, R. E.; Chia, F.; Conte, E.; Cook, A.; Hadfield, M.; Haslbeck, E.; Holm, E.; Kavanagh, C.; Kohrs, D.; Kovach, B.; Lee, C.; Mazzella, L.; Meyer, A. E.; Qian, P.; Sawant, S. S.; Schultz, M.; Sigurdsson, J.; Smith, C.; Soo, L.; Terlizzi, A.; Wagh, A.; Zimmerman, R.; Zupo, V. Biofouling and barnacle adhesion data for fouling-release coatings subjected to static immersion at seven marine sites. *Biofouling* **2000**, *16*, 331−344.
(33) Lim, J. Y.; Tay, T. S.; Lim, C. S.; Lee, S. S. C.; Teo, S. L. M.; Tan, K. S. Mytella strigata (Bivalvia: Mytilidae): an alien mussel recently introduced to Singapore and spreading rapidly. *Molluscan Res.* **2018**, *38*, 170−186.
(34) Kim, P.; Galhenage, T. P.; Lomakin, J. Curable polysiloxane compositions and slippery materials and coatings and articles made therefrom. U.S. Patent 10240067B2, 2019.
(35) Kim, P.; Galhenage, T. P.; Lomakin, J. Curable polysiloxane compositions and slippery materials and coatings and articles made therefrom. U.S. Patent 2018327684A1, 2018.
(36) Marchuk, I.V.; Cheverda, V.V.; Strizhak, P.A.; Kabov, O.A. Determination of surface tension and contact angle by the axisymmetric bubble and droplet shape analysis. *Thermophys. Aeromech.* **2015**, *22*, 297−303.
(37) Girifalco, L. A.; Good, R. J. A theory for the estimation of surface and interfacial energies. I. Derivation and application to interfacial tension. *J. Phys. Chem.* **1957**, *61*, 904−909.
(38) Owens, D. K.; Wendt, R. C. Estimation of the surface free energy of polymers. *J. Appl. Polym. Sci.* **1969**, *13*, 1741−1747.
(39) Basu, S.; Hanh, B. M.; Isaiah Chua, J.Q.; Daniel, D.; Ismail, M. H.; Marchioro, M.; Amini, S.; Rice, S. A.; Miserez, A. Green Biolubricant Infused Slippery Surfaces to Combat Marine Biofouling. *J. Colloid Interface Sci.* **2020**, *568*, 185−197.
(40) Oyen, M. L. Nanoindentation of biological and biomimetic materials. *Exp. Technol.* **2013**, *37*, 73−87.
(41) Caporaso, J. G.; Lauber, C. L.; Walters, W. A.; Berg-Lyons, D.; Lozupone, C. A.; Turnbaugh, P. J.; Fierer, N.; Knight, R. Global patterns of 16S rRNA diversity at a depth of millions of sequences per sample. *Proc. Natl. Acad. Sci. U. S. A.* **2011**, *108*, 4516−4522.
(42) Callahan, B. J.; McMurdie, P. J.; Rosen, M. J.; Han, A. W.; Johnson, A. J. A.; Holmes, S. P. DADA2: High-resolution sample inference from Illumina amplicon data. *Nat. Methods* **2016**, *13*, 581−583.
(43) McMurdie, P. J.; Holmes, S. phyloseq: An R package for reproducible interactive analysis and graphics of microbiome census data. *PLoS One* **2013**, *8*, e61217.
(44) Oksanen, J.; Blanchet, F. G.; Kindt, R.; Legendre, P.; Minchin, P. R.; O'Hara, R.; Simpson, G. L.; Solymos, P.; Stevens, M.; Wagner, H. *vegan: Community Ecology R Package*, 2013.
(45) Wong, T.-S.; Kang, S. H.; Tang, S. K. Y.; Smythe, E. J.; Hatton, B. D.; Grinthal, A.; Aizenberg, J. Bioinspired Self-Repairing Slippery Surfaces with Pressure-Stable Omniphobicity. *Nature* **2011**, *477*, 443−447.
(46) Delmas, M.; Monthioux, M.; Ondarçuhu, T. Contact Angle Hysteresis at the Nanometer Scale. *Phys. Rev. Lett.* **2011**, *106*, 136102.
(47) Tanneberger, K.; Knöbel, M.; Busser, F. J. M.; Sinnige, T. L.; Hermens, J. L. M.; Schirmer, K. Predicting fish acute toxicity using a fish gill cell line-based toxicity assay. *Environ. Sci. Technol.* **2013**, *47*, 1110−1119.
(48) Sakai, T.; Kurakazu, M.; Akagi, Y.; Shibayama, M.; Chung, U.-i. Effect of swelling and deswelling on the elasticity of polymer networks in the dilute to semi-dilute region. *Soft Matter* **2012**, *8*, 2730−−2736.
(49) Al-Barwani, S. M.; Arshad, A.; Amin, S. M. N.; Japar, S. B.; Siraj, S. S.; Yap, C. K. Population dynamics of green mussel Perna viridis from the high spat-fall coastal water of Malacca, Peninsular Malaysia. *Fish Res.* **2007**, *84*, 147−152.
(50) Kavanagh, C. J.; Swain, G. W.; Kovach, B. S.; Stein, J.; Darkangelo-Wood, C.; Truby, K.; Holm, E.; Montemarano, J.; Meyer, A.; Wiebe, D. The effects of silicone fluid additives and silicone elastomer matrices on barnacle adhesion strength. *Biofouling* **2003**, *19*, 381.

https://dx.doi.org/10.1021/acsapm.0c00916
ACS Appl. Polym. Mater. 2020, 2, 5147−5162

(51) Leonardi, A. K.; Ober, C. K. Polymer-Based Marine Antifouling and Fouling Release Surfaces: Strategies for Synthesis and Modification. *Annu. Rev. Chem. Biomol. Eng.* **2019**, *10*, 241−264.
(52) Grinthal, A.; Aizenberg, J. Mobile Interfaces: Liquids as a Perfect Structural Material for Multifunctional, Antifouling Surfaces. *Chem. Mater.* **2014**, *26*, 698−708.
(53) Peppou-Chapman, S.; Neto, C. Mapping Depletion of Lubricant Films on Antibiofouling Wrinkled Slippery Surfaces. *ACS Appl. Mater. Interfaces* **2018**, *10*, 33669−33677.
(54) Fletcher, M.; Marshall, K. C. Are solid surfaces of ecological significance to aquatic bacteria? *Adv. Microb. Ecol.* **1982**, *6*, 199−230.
(55) Liu, Y.; Zhao, Q. Influence of surface energy of modified surfaces on bacterial adhesion. *Biophys. Chem.* **2005**, *117*, 39−45.
(56) Harder, T.; Yee, L. Bacterial adhesion and marine fouling. In *Advances in Marine Antifouling Coatings and Technologies*; Hellio, C., Yebra, D., Eds.; Woodhead: Cambridge, UK, 2009; pp 113−125.
(57) Steinberg, P. D.; De Nys, R.; Kjelleberg, S. Chemical Cues for Surface Colonization. *J. Chem. Ecol.* **2002**, *28*, 1935.
(58) Wheeler, G. L.; Tait, K.; Taylor, A.; Brownlee, C.; Joint, I. Acyl-homoserine lactones modulate the settlement rate of zoospores of the marine alga Ulva intestinalis via a novel chemokinetic mechanism. *Plant, Cell Environ.* **2006**, *29*, 608.
(59) Tait, K.; Williamson, H.; Atkinson, S.; Williams, P.; Camara, M.; Joint, I. Turnover of quorum sensing signal molecules modulates cross-kingdom signalling. *Environ. Microbiol.* **2009**, *11*, 1792−1802.
(60) Chung, H. C.; Lee, O. O.; Huang, Y. L.; Mok, S. Y.; Kolter, R.; Qian, P. Y. Bacterial community succession and chemical profiles of subtidal biofilms in relation to larval settlement of the polychaete Hydroides elegans. *ISME J.* **2010**, *4*, 817−828.
(61) Callow, M. E.; Callow, J. A. Marine biofouling: a sticky problem. *Biologist* **2002**, *49*, 10−4.
(62) Hellio, C.; Yebra, D. M. *Advances in Marine Antifouling Coatings and Technologies*; Woodshead Publishing: Cambridge, U.K., 2009; p 1.
(63) Petrone, L. Molecular surface chemistry in marine bioadhesion. *Adv. Colloid Interface Sci.* **2013**, *195*−*196*, 1−18.
(64) Rittschof, D.; Costlow, J. D. Bryozoan and barnacle settlement in relation to initial surface wettability: A comparison of laboratory and field studies. *Sci. Mar.* **1989**, *53*, 411.
(65) Petrone, L.; Di Fino, A.; Aldred, N.; Sukkaew, P.; Ederth, T.; Clare, A. S.; Liedberg, B. Effects of surface charge and Gibbs surface energy on the settlement behaviour of barnacle cyprids (*Balanus amphitrite*). *Biofouling* **2011**, *27*, 1043−1055.
(66) Wei, W.; Yu, J.; Broomell, C.; Israelachvili, J. N.; Waite, J. H. Hydrophobic enhancement of dopa-mediated adhesion in a mussel foot protein. *J. Am. Chem. Soc.* **2013**, *135*, 377−383.
(67) Yu, J.; Kan, Y.; Rapp, M.; Danner, E.; Wei, W.; Das, S.; Miller, D. R.; Chen, Y.; Waite, J. H.; Israelachvili, J. N. Adaptive Hydrophobic and Hydrophilic Interactions of Mussel Foot Proteins with Organic Thin Films. *Proc. Natl. Acad. Sci. U. S. A.* **2013**, *110*, 15680−15685.
(68) Waite, J. H. Mussel adhesion−essential footwork. *J. Exp. Biol.* **2017**, *220*, 517−530.
(69) Petrone, L.; Kumar, A.; Sutanto, C. N.; Patil, N. J.; Kannan, S.; Palaniappan, A.; Amini, S.; Zappone, B.; Verma, C.; Miserez, A. Mussel adhesion is dictated by time-regulated secretion and molecular conformation of mussel adhesive proteins. *Nat. Commun.* **2015**, *6*, 8737.
(70) Rana, D.; Matsuura, T. Surface Modifications for Antifouling Membranes. *Chem. Rev.* **2010**, *110*, 2448−2471.

https://dx.doi.org/10.1021/acsapm.0c00916
ACS Appl. Polym. Mater. 2020, 2, 5147−5162